Toxicology Research

Accepted Manuscript

ROYAL SOCIETY OF CHEMISTRY

www.rsc.org/toxicology

Cite this: DOI: 10.1039/c0xx00000x

www.rsc.org/toxicology

PAPER

Metabolomic Profiling of Emodin-induced Cytotoxicity in Human Liver Cells and the Mechanism Study

Xiaoyan Liu[a,b], Yanqiu Liu[a,c], Yang Qu[a,d], Mengchun Cheng[a], Hongbin Xiao[a,e,*]

Received (in XXX, XXX) Xth XXXXXXXXX 20XX, Accepted Xth XXXXXXXXX 20XX

DOI: 10.1039/b000000x

Emodin is one of the most representative natural anthraquinone polyphenols and the liver is one of the major target organs for drug-induced toxicology. The hepatocyte is frequently affected due to its role in emodin metabolism and accumulation. Although the hepatotoxicity of emodin has been reported, its toxicological mechanism is still unclear. The purpose of the present study was to evaluate the cytotoxicity of emodin in cultured human normal liver cells (L-02), to investigate the toxicity-related metabolic pathways and to predict the possible toxicity mechanism. Cell viability was analyzed by 3-(4, 5-dimethylthiazol-2yl)-2, 5-diphenyltetrazolium bromide (MTT) assay. Cytotoxicity tests demonstrated a concentration-dependent toxic effect of emodin on L-02 cells. Cells were treated for 48 h with low, medium and high doses of emodin, respectively. And then subjected to metabolomics analysis using ultra-high performance liquid chromatography-tandem mass spectrometric (UPLC-MS). Intracellular metabolomics analysis revealed that emodin significantly disturbed cellular glutathione and fatty acid metabolism. In addition, emodin-cysteine adduct was firstly identified in cell cultured medium, and the level of it was increased with increasing concentrations of emodin. The possible relationship among metabolism disorders, adduct formation and emodin hepatotoxicity was also discussed. This study provides the new insight into the cytotoxicity of emodin on metabolic pathways in human liver cells.

1 Introduction

Emodin, a natural anthraquinone polyphenol distributed in several popular Chinese herbal medicines including *Rheum palmatum, Polygonum multiflorum, Cassia acutifolia and Aloe vera*, has a wide range of therapeutic applications, including a reducing agent in type 2 diabetes[1, 2] and an anticancer agent in various cancers such as pancreas et,al[3, 4]. However, its side-effects, such as genotoxicity[5, 6], embryonic toxicity[7] and nephrotoxicity[8] have been reported in the past few decades. Moreover, it has been revealed to cause *in vivo* hepatotoxicity[9, 10].

Using well-designed *in vitro* assays is now an efficient approach for predicting chemicals' toxicity to humans, which would facilitate the mechanism understanding of the mode of action. In previous studies, the cytotoxicity of chemicals such as perfluorooctanoic acid and pyrrolizidine has been researched in human liver cells[11, 12]. Emodin-induced cell injury has been disclosed via disrupting mitochondrial function [13], regulating protein kinase C expression[14, 15] and inducing DNA damage [16]. However, only few studies focus on the mechanism of emodin-induced hepatocyte cytotoxicity. A recent study revealed that accumulation of emodin in hepatocyte cytoplasm could contribute to hepatocyte injury [17].

Drug-induced cytotoxicity is related to cell metabolism. Metabolomic is an omics technology that enables cellular functions to be analyzed via a holistic view of metabolic pathways. Of several metabolic detection techniques, liquid chromatography–mass spectrometry (LC-MS) suits the simultaneous profiling of lipid-related metabolic pathways, e.g., fatty acids, steroids, phospholipids and acylcarnitine pathways[18, 19]. In this study, an UPLC-MS-based metabolomics approach was applied to the study of emodin-disturbed hepatocyte metabolism. L-02, one of the commonly used human normal liver cell lines for in vitro evaluation cytotoxicity that induced by drugs, was chosen as the model system to evaluate the hepatotoxicity of emodin. Such as, Ma and colleagues and some other researchers' studies showed that this cell line is fit to analysis of drug-induced hepatotoxicity [20, 21, 22].

The primary goal of this study was to investigate emodin-induced cytotoxicity in human normal liver cells (L-02), to assess the toxicity-related metabolic pathways and to explore toxicity-related mechanism. Cell viability was determined using MTT assay. After cultivated for 48 h with different doses of emodin (low, medium and high), respectively, the intracellular metabolites in cell samples were extracted for subsequent metabolomics study, and the corresponding cell cultured medium was prepared for emodin-cysteine adduct analysis. The formation of emodin-cysteine adduct in liver cells may contribute to emodin-induced metabolic disorder. Our findings provide insights into the mechanism of emodin-induced hepatotoxicity, and are potentially of clinical significance to diagnose emodin-induced hepatotoxicity.

2 Materials and methods

2.1 Materials

Methanol and acetonitrile (HPLC grade) were obtained from Sigma-Aldrich (St. Louis, MO, USA). Formic acid (HPLC grade) was purchased from Kemiou (Tianjin, China). Roswell Park Memorial Institute-1640 (RPMI-1640) medium and fetal bovine serum (FBS) was obtained from Gibco (Grand Island, N.Y, USA). 3-(4, 5-dimethylthiazol-2yl)-2, 5-diphenyltetrazolium bromide (MTT), dimethylsulfoxide (DMSO) and Bradford protein measurement kit were purchased from Solarbio (Beijing, China). Emodin (CAS No. 518-82-1, 98% purity), was obtained from National Institutes for Food and Drug Control (Beijing, China). Reverse osmosis deionized glass distilled water was obtained in house using a Milli-Q system with a 0.22 μm Millipore filter (Millipore, USA).

2.2 Cell culture

Human normal liver cells (L-02; obtained from Shanghai Obio Biotech. Corp., Ltd, Shanghai, China) were cultured at 37 ℃ in RPMI-1640 medium supplemented with 10% FBS (Gibco, Grand Island, N.Y, USA) in a humidified 5% CO_2 atmosphere. The cells were detached using cell scrapper for metabolomics experiment [23].

2.3 Cell viability assay

MTT assay was used to measure cell viability. Equal number of L-02 cells (10^6/ml) was seeded into 96-well plates (3 replicates for each concentration). Cells were cultivated for 24 h and were then treated for 48 h with series of concentrations of emodin in fresh cultured medium ranged from 10 to 120 μM, respectively. Cells with non-emodin medium served as control and medium without cells served as blank. Then, 15 μl of MTT (5 mg/ml) was added to each well and incubation was continued for 4 h at 37 ℃. After discarding the medium, the formazan products were dissolved with 150 μl DMSO and the optical density (OD) values at 570 nm were determined using a Sunrise micro plate absorbance reader (TECAN. Austria). Inhibition rates of emodin were calculated using following equation. And the inhibition ratio curve of emodin was depicted using Graphpad Prim (version 5.0, Intuitive Software for Science, San Diego, CA, USA) accordingly.

$$Inhibition\ rate = \frac{OD_{570control} - OD_{570dosed}}{OD_{570control} - OD_{570blank}} \times 100\%$$

2.4 Assay for intracellular metabolomics study

Equal number of L-02 cells (10^6/ml, 2 ml) was seeded into 6-well plates (6 replicates for each group). Cells were cultivated for 24 h and were then treated for 48 h with the different concentrations (10 μM, 20 μM and 30 μM) of emodin in fresh cultured medium. Vehicle-treated cells (treated with medium) served as control, and blank medium with emodin (without cells) served as blank control. Cells were quenched using 1 ml chilled methanol, washed three times with 50 mM phosphate buffered saline (PBS, pH 7.4), washed once with water to remove saline solution, scrapped by cell scraper, centrifuged at 92 ×g for 5 min to obtain cell pellets, and stored at -80℃ until further analysis.

The method of metabolite extraction was described in previous research with little modifications [23]. Briefly, 200 μl of chilled 80% (v/v) methanol solution was added to quench the enzymatic reactions. Cell lysate was prepared with homogenization using the mini-beadbeater 16 (Biospec, USA) (homogenization for 1min, internal for 20s, twice), and centrifuged at 4℃, 20, 627 ×*g* for 10 min. The supernatant was dried under vacuum and then reconstituted with 100 μl of 5% acetonitrile. The protein precipitated in each sample was quantified using Bradford protein measurement kit (Solarbio, China) according to manufacturer instructions. The total protein contents were used to calibrate the slight differences in the number of cells among different groups. A quality control (QC) sample was prepared by mixing 20 μl aliquots of each sample. The samples were stored at -80℃ prior to LC-MS analysis.

The UPLC-MS analysis was carried out using an Agilent 1290 ultra performance liquid chromatography system coupled with Agilent 6520 time-of-flight mass spectrometry, using a Zorbax Eclipse plus C18 column (RRHD1.8 μm, 3.0×150 mm; Agilent, USA). The column temperature was maintained at 50 ℃, and the injection volume was 5 μl. The separation was performed using a gradient program with water (solvent A, modified by the addition of 0.1% formic acid) and acetonitrile (solvent B). The pump flow rate was 0.3 ml/min with an initial solvent composition of 5% B. The gradient was conducted from 5- 50% B over 3 min, 50-100% B over 3-15 min, held at 100% B for 5min, decreased to 5% B within 1 min, and held at 5% B for 5 min .To ensure the repeatability and stability of the instrument, QC sample was analyzed twice prior to the first initial injection, and analyzed once every eight sample injections during analysis process. All samples were injected randomly.

Mass spectrometry and accurate mass acquisition were operated in electrospray ionization mode. The optimal capillary voltage and the cone voltage were set at 3.5 kV and 40 V, respectively. The nebulization gas flow rate was set at 8 L/min and the liquid nebulizer was set at 40 psig. The capillary temperature was set at 350℃. Data were acquired at a rate of 1 spectrum per second for MS and 3 spectra per second for MS/MS (centroid mode). The collision energy for MS/MS was 10, 20 or 40 eV according to the properties of metabolites. The mass scan range was from 100 to 1000 for MS and 30 to 1000 for MS/MS. The real-time correction method was used to increase the accuracy and stability of the mass.

2.5 Emodin-Cysteine analysis and identification

The cell cultured medium was centrifuged at 1467 ×*g* for 10 min to remove debris. A 200 μl aliquot of cell cultured medium was taken into a 1.5 ml centrifuge tube. Then, 400 μl of acetonitrile was added, and the mixture was oscillated for 5 min, stand for 30 min at 4 ℃ and centrifuged at 20,627 ×*g* for 10 min to remove protein. The supernatant was dried under vacuum and reconstituted with 100 μl of 5% acetonitrile. A quality control (QC) sample was prepared by mixing 20 μl aliquots of each sample to ensure the stability of the instrument. The instrumental analysis method was identical with that mentioned in Section 2.4. The identification of emodin-cysteine adduct was based on the accurate mass matching, MS/MS fragment explanation and chemical synthesis result comparison.

Cite this: DOI: 10.1039/c0xx00000x

www.rsc.org/toxicology

PAPER

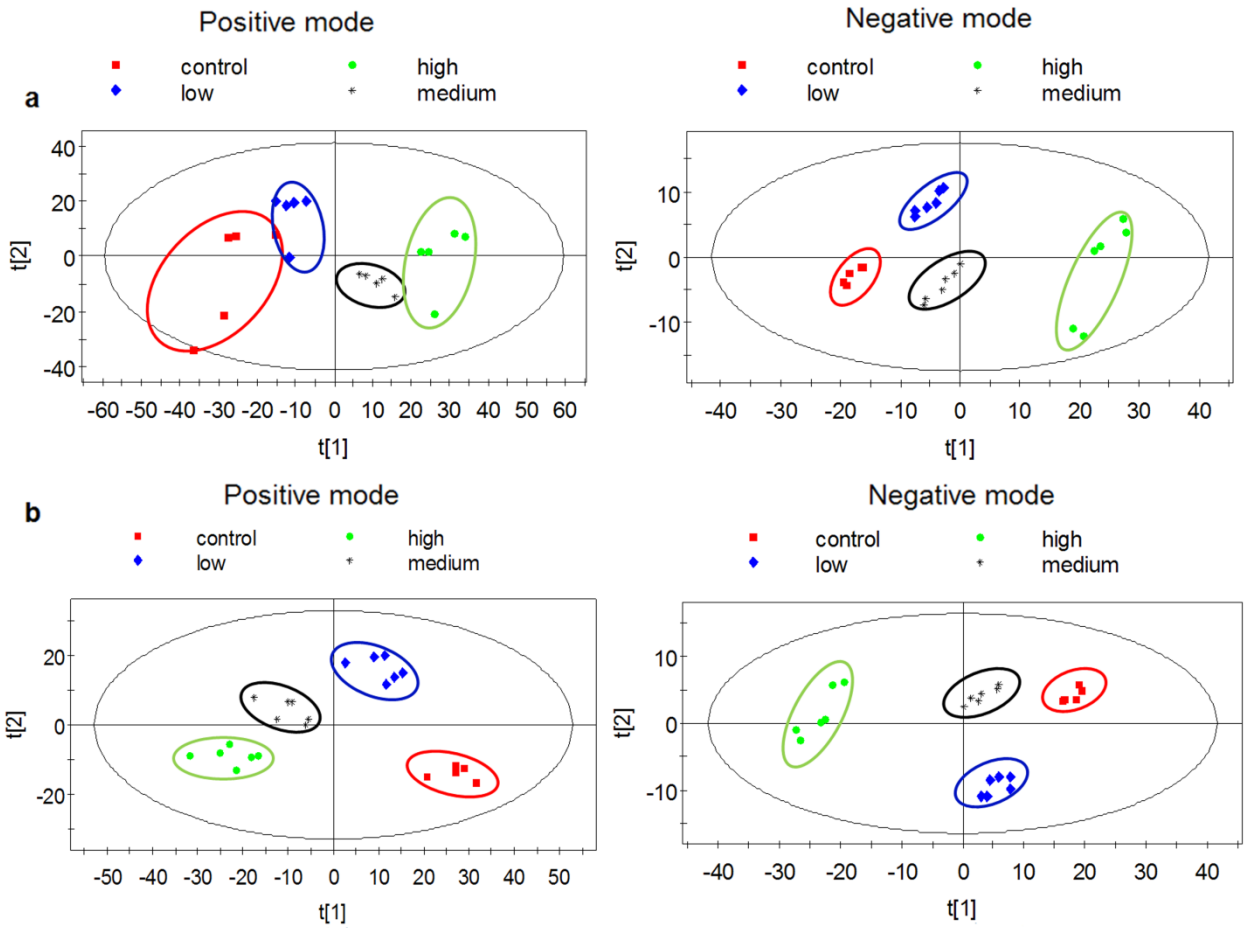

Fig.1 Metabolomic profiles of the control and emodin-treated groups in positive and negative mode using UPLC-MS system. **(a)** PCA scatter plot. **(b)** PLS-DA scatter plot (Positive mode, R^2X, 0.719; R^2Y, 0.989; Q^2 (cum), 0.899; negative mode, R^2X, 0.872; R^2Y, 0.98; Q^2 (cum), 0.967). The artwork was created using SIMCA-P 11.0 (Umetrics, Sweden) software.

2.6 Analysis of metabolomics data

Raw data were analyzed using XCMS online [24], which follows typical data processing steps, including peak discrimination, peak filtering, peak alignment, noise elimination and the generation of a matrix that consisted of the retention time, m/z value and the peak areas. Peak areas were firstly calibrated by protein quantification coefficient to eliminate cells number inference and then normalized by probabilistic quotient normalization (PQN), log transformation and Pareto scaling to make features more comparable. Variables, whose CV% (Coefficients of variations) were more than 30% (CV% were calculated based on QC data), were removed from further statistical analysis [25].

Pattern recognition analysis (principal component analysis, PCA; partial least squares discriminate analysis, PLS-DA) was carried out using SIMCA-P 11.0 (Umetrics, Sweden) software. Student's t test (two-tailed) was used for statistical comparisons. The relative concentration of differential metabolites was expressed in a heatmap. Data analysis and heatmap visualization was conducted using Graphpad Prism (version 5.0, Intuitive Software for Science, GraphPad Software company, San Diego, CA, USA) and MeV software (version 4.9.0, Dana-Farber Cancer Institute, Boston, MA, USA), respectively.

The identification of the significant metabolites was performed based on the published identification strategy [26]. The following steps were carried out. First, the quasimolecular ions were confirmed according to extracted ions chromatogram (EIC). Second, the exact masses of monoisotopic molecular weights were used to search our in-house human metabolites fluid database and the free online databases, including METLIN (http://metlin.scripps.edu), HMDB (http://www.hmdb.ca/), ChemSpider (http://www.chemspider.com), KEGG (http://www.genome.jp) and Lipid Maps (http://www.lipidmaps.org). The mass tolerance was set as 10 ppm, and several candidates could be selected for each

quasimolecular ion. The third step was to determine the exact structure of each biomarker metabolite through commercial standards comparison or MS/MS spectra analysis and spectra databases comparison.

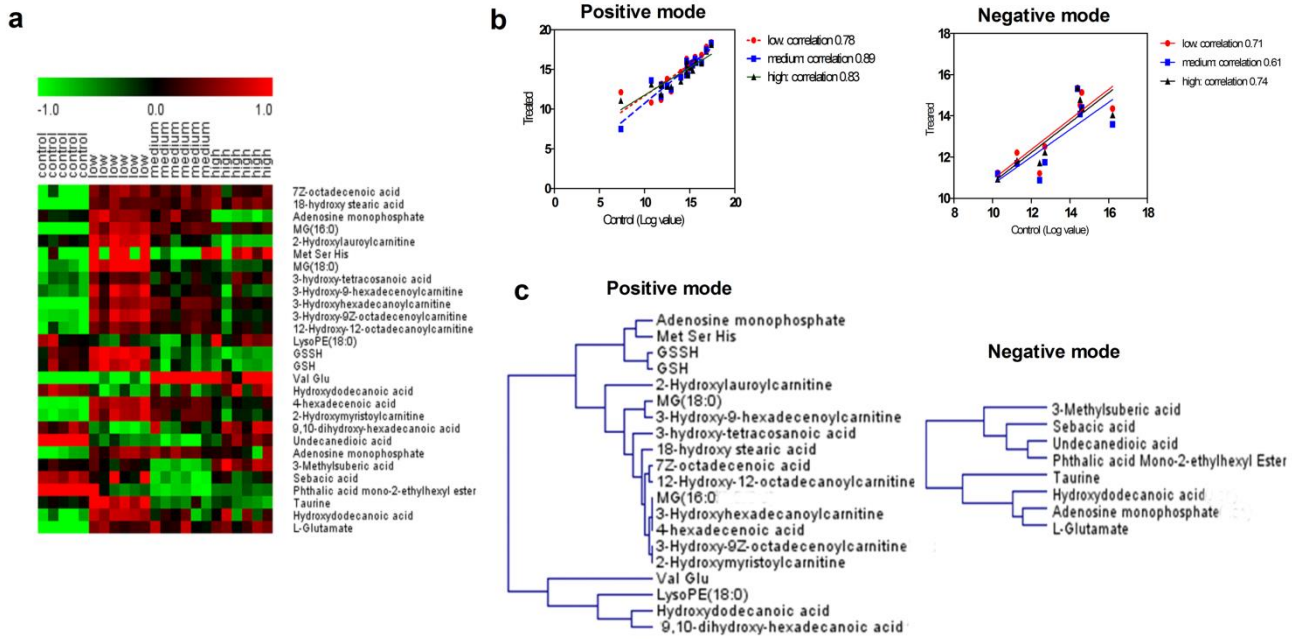

Fig.2 Significant changed metabolites in emodin-treated liver cells. **(a)** Heat map showing differential metabolites in emodin treated liver cells relative to control liver cells. **(b)** Correlation plots for metabolites altered at low, medium and high doses of emodin treatment in L-02 cells. **(c)** Dendrogram representing hierarchical clustering of the emodin toxicity related metabolites described in **a**. Heat map and dendrogram were created using MeV software (version 4.9.0, Dana-Farber Cancer Institute, Boston, MA, USA), and correlation plots were plotted using Graphpad Prism (version 5.0, Intuitive Software for Science, San Diego, CA, USA).

3 Results

3.1 Cell viability

A dose-dependent increase in L-02 cell inhibition rates was observed with increasing emodin concentrations (ESM_1). IC50 value was calculated as 30 μM for 48 h using Graphpad prism 5.0. And therefore, the doses used in this study were set as 10, 20, 30 μM (low, medium and high doses), for higher doses could induce larger death rate (larger than 50%) of cells and would cause larger deviations for further analysis The morphologies of the adherent L-02 cells after exposure to 10, 20, 30 μM emodin for 48 h were shown in ESM_2. Untreated L-02 cells appeared to be in spindle-like shapes and in high density distribution in the flasks, while L-02 cells treated with emodin became gradually contracted and rounded, and the density of the adherent cells became lower with increasing emodin concentrations.

3.2 Overview of metabolic profiling

The metabolic profiles of L-02 cells were acquired under both positive and negative ionization mode using UPLC-TOF-MS. QC sample was used to ensure the quality of the metabolomics data (ESM_3). A good separation between the control and dosed groups was observed when using unsupervised principal component analysis (PCA) (Fig.1a). Clearer results could be obtained from the score plot of PLS-DA (Fig.1b) (Positive mode, R^2X, 0.719; R^2Y, 0.989; Q^2(cum), 0.899; negative mode, R^2X, 0.872; R^2Y, 0.98; Q^2 (cum), 0.967). These results indicated distinct metabolic differences between the control and emodin-treated groups.

According to variable importance in the projection (VIP) values obtained from PLS-DA models, 80 features in positive mode and 30 features in negative mode were selected as potential cytotoxicity-related biomarkers. After manual validation, 23 features of them were found as isotope ions. Finally, 28 features (26 metabolites) were identified and semi-quantified (Table S1, Fig.2a and ESM_4).

To further analyze emodin hepatotoxicity related metabolic pathways, hierarchical clustering and correlation analysis were performed on identified biomarkers. Interestingly almost all the marker metabolites showed a consistent pattern of change at low, medium and high doses treatment (Fig.2b), which indicated the close metabolic relevance of these biomarkers. In addition, hierarchical clustering analysis further ensured the close metabolic relevance (Fig.2c).

3.2.1 Changes in glutathione metabolism

Emodin caused glutathione metabolism disorder in L-02, marked by the decreased level of glutathione (GSH), oxidized glutathione (GSSH) and the increased level of the metabolite of GSH, glutamate (Fig.3a). The levels of glutathione-related metabolites were gradually decreased or increased with increasing emodin concentration, and at high concentration point, the change ranges of metabolites became small when compared to medium dose group (Fig.3a). These results suggested that a drastic disturbance of GSH metabolism occurred with emodin treatment and the degree of emodin-induced injury would gradually reach to a maximum with increasing concentration of emodin. GSH is a critical cellular antioxidant. After GSH depletion, the toxicity of

drugs and chemicals enhanced [27]. Oxidative stress and peroxidation will be subsequently happened resulting from GSH depletion. Moreover, cellular energy metabolism was also affected by emodin treatment, for increased level of adenosine monophosphate (AMP) suggested a increased ATP utilization of cells [28].

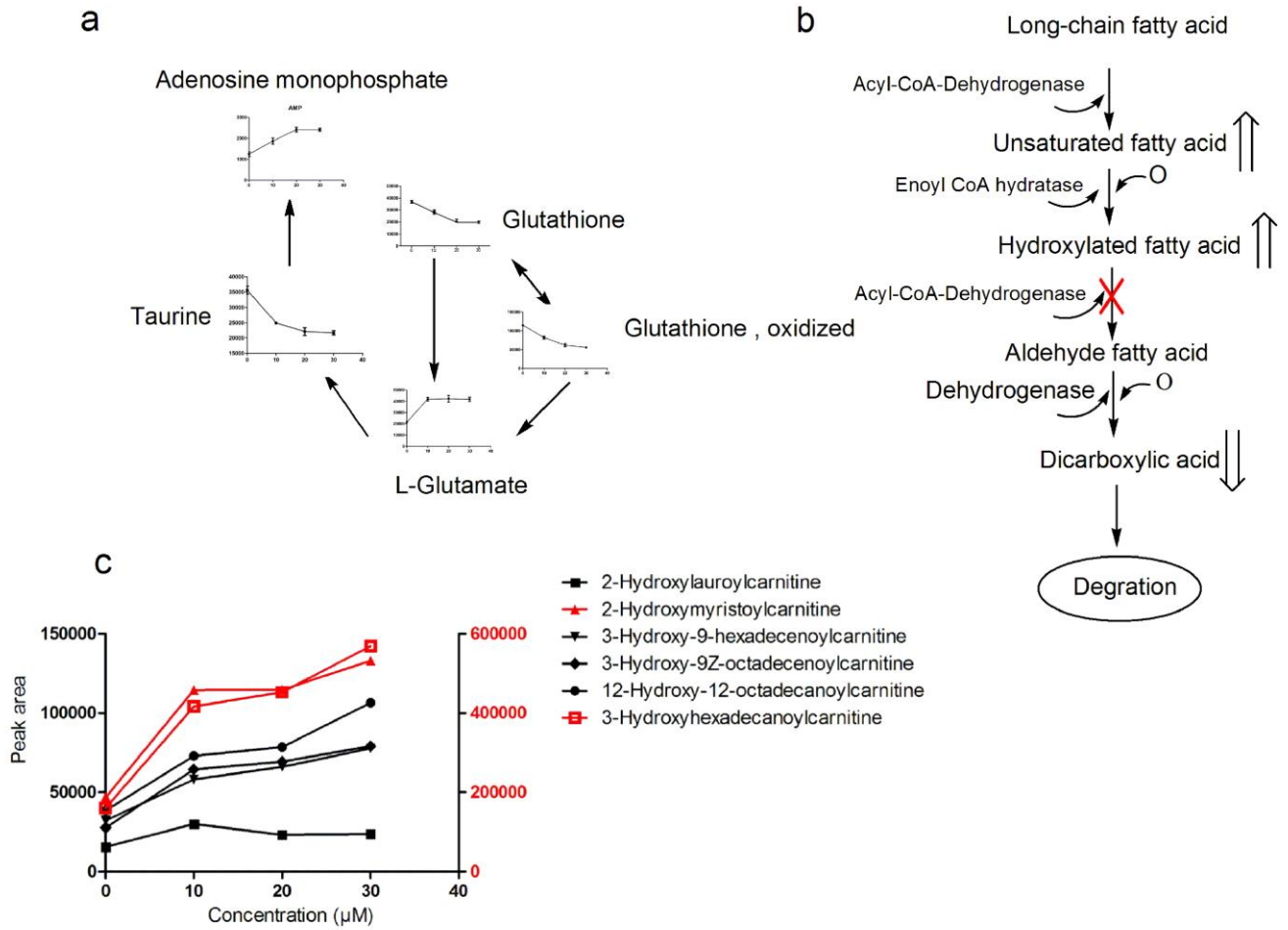

Fig.3 Disturbance of metabolic pathways induced by emodin. **(a)** Changes of metabolites in glutathione metabolism. **(b)** Disturbance of fatty acid oxidation induced by emodin (The double-line arrow represents the increased or decreased levels of the metabolites). **(c)** Changes of metabolites in acylcarnitine metabolism.

3.2.2 Changes in fatty acid metabolism

Fatty acid metabolism disorders, including fatty acid oxidation and acylcarnitine metabolism, were occurred in L-02 cells with emodin cytotoxicity. Under normal conditions, long-chain fatty acid oxidation involves several steps as follows; the first step is the oxidation of the fatty acid by acyl-CoA-dehydrogenase. The enzyme catalyzes the formation of a double bond; the next step is the hydration of the double bond; the third step is the oxidation of hydroxyacyl-CoA by NAD^+. This process converts the hydroxyl group into aldehyde group; the final step is the formation of dicarboxylic acid and the cleavage of ketoacyl CoA by the thiol group of another molecule of CoA. However, these normal metabolism processes were disturbed by emodin. The levels of hydroxylated fatty acids, including hydroxydodecanoic acid, 18-hydroxy stearic acid, 9, 10-dihydroxy-hexadecanoic acid and 3-hydroxy-tetracosanoic acid were gradually increased with increasing emodin concentration. These results prompted us to predict that the third step of fatty acid oxidation process was blocked with emodin treatment. This speculation was further ensured by the increased levels of metabolites, including 4-hexadecenoic acid, 7Z-octadecenoic acid produced in the first oxidation step and the decreased levels of metabolites produced in the latter step, including undecanedioic acid and sebacic acid (Fig.3b).

In addition, significant changes of acylcarnitines in emodin treated groups further validated the deduction that fatty acid metabolism disorder occurred in L-02 cells. After emodin treatment, levels of acylcarnitines showed statistically significant increased (Fig.3c). Acylcarnitines are essential for fatty acid metabolism. They help the activated long-chain fatty acids to be transported into mitochondria and then be oxidized to acetyl-CoA. Moreover, as specific substrates of mitochondrial β-oxidation, acylcarnitines play an important role in mitochondrial function, and mitochondrial dysfunction is reported to be associated with hepatotoxicity [29]. Acylcarnitines can facilitate the transfer of long-chain fatty acids from cytoplasm into mitochondria during the oxidation of fatty acids, and the levels of them are the rate-limiting step in fatty acid β-oxidation[30, 31]. Our current results suggested that emodin had the potential to disturb fatty acid metabolism in L-02 cells through affecting fatty acid

transportation and oxidation in liver cells.

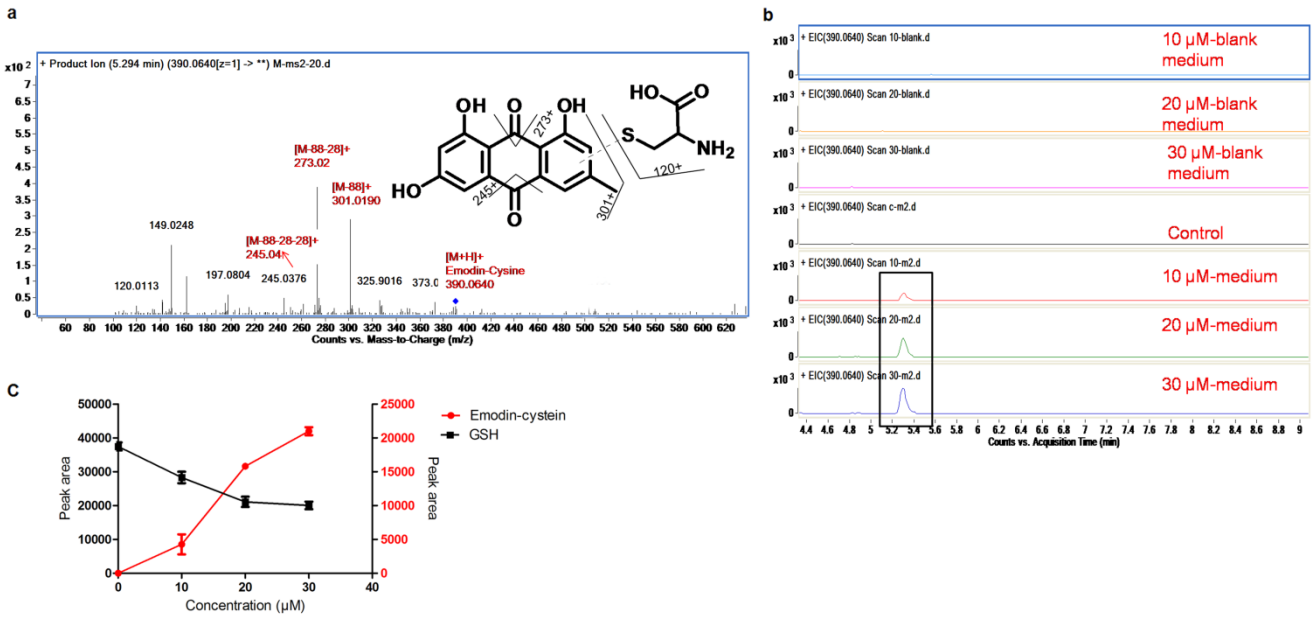

Fig.4 Emodin-cysteine adduct analysis and identification. **(a)** MS^2 fragmentation of emodin-cysteine. **(b)** Extracted ion chromatogram of emodin-cysteine adduct. **(c)** Dose-dependent changes of glutathione (GSH) and emodin-cysteine adduct.

3.3 Emodin-cysteine formation and identification

Emodin-cysteine adduct was identified in cell cultured medium (Fig.4a). Fragment ions of 301.02, 273.02 and 245.04 are the characteristic fragments of emodin and the fragment of 120.01 is the characteristic fragment of cysteine. Additionally, the structure of this adduct was further validated through comparison with standard obtained from chemical synthesis，which using DMSO as the solubilizing agent. And the detailed synthesis procedure was given in supplementary materials (ESM_5). The level of emodin-cysteine adduct was increased with increasing emodin concentration (Fig.4b and Fig.4c). Since the CV% of the adduct peak area in QC data was less than 30% (CV, 7.5%), the differences among different groups were proved more likely to reflect biological changes rather than analytical variations. However, in blank medium (medium without liver cells) with different concentrations of emodin, emodin-cysteine was not detected (Fig.4b), and within L-02 cells it was also not detected. These results suggested that emodin-cysteine adduct was initially formed within liver cells, and finally secreted into the cultured medium. The formation of this adduct would result in the depletion of intracellular cysteine, which is an essential material of GSH synthesis. GSH synthesis disorder (Fig.4c) would contribute to a series of cellular metabolism disorders, including oxidation stress and fatty acid metabolism. Taken together, the formation of emodin-cysteine adduct was suspected to be related to emodin induced hepatotoxicity.

4 Discussions

The UPLC-MS metabolome analysis demonstrated that emodin had the potential to disturb GSH and fatty acid metabolism in human liver cells, through which produced hepatotoxicity. The discovery of a new adduct, emodin-cysteine, facilitated us to proposed one mechanism related to emodin-induced hepatotoxicity.

Liver is the essential organ for drugs and xenobiotics metabolism. Drug-induced hepatotoxicity could result from the direct toxicity of the parent compound or the indirect toxicity of more active metabolites. For example, acetaminophen hepatotoxicity begins with metabolism of the parent compound to the reactive electrophile N-acetyl-p-benzoquinone imine (NAPQI). Then NAPQI depletes GSH and produces hepatotoxicity[32, 33]. Ethanol hepatotoxicity begins with reactive oxygen species (ROS) produced in CYP2E1-dependent ethanol metabolism [34]. The mechanism of emodin hepatotoxicity is rarely reported. The present study suggested an indirect toxicity mechanism of emodin. Emodin is firstly drawn into the liver cells, and binds to cysteine through the function of thioltransferase. Emodin links to cysteine to form a cysteine adduct which is then released to the cultured medium. This combination will 'spend' cellular cysteine, which is the necessary metabolite to glutathione (GSH) synthesis. GSH synthesis plays a central role in cell protection, and GSH depletion will cause a series of metabolism disorders, including oxidative stress and fatty acid oxidation disorder. In addition, synthesis of some proteins containing cysteine will be blocked due to cysteine depletion. All these series of metabolic disorders will consequently contribute to the death of liver cells (Fig.5).

The limitation of our study is that we only detected emodin-cysteine adduct in the cultured medium. However, it must exist within liver cells within a certain period of time or one time point, since it cannot be formed in blank cultured medium. Therefore, capturing the initial formation of the adduct remains to be investigated. Nevertheless, the results in present study will help with better understanding the mechanism of emodin induced hepatotoxicity. Also, several intracellular metabolites and emodin-cysteine adduct could used as biomarkers for emodin

hepatotoxicity.

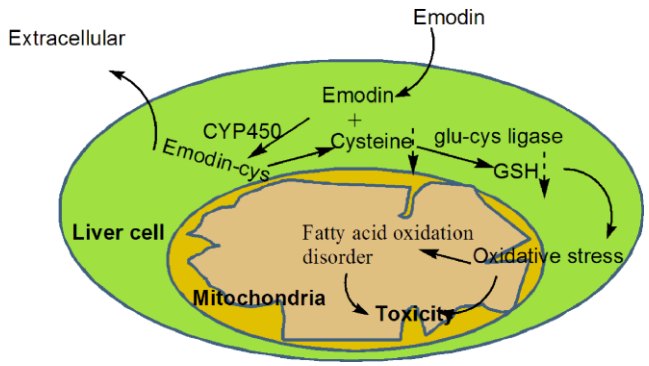

Fig.5 Probable toxicity mechanism of emodin in liver cells. The dotted arrows represent the up- or down-regulation of metabolites.

5 Concluding remarks

In conclusion, the present study identified emodin hepatotoxicity related metabolic pathways, including GSH metabolism and fatty acid metabolism and discovered a new emodin-cysteine adduct formed in liver cells. A new indirect toxicity mechanism of emodin was proposed. As far as we know, there is no study that has investigated the changes in the intracellular metabolites during emodin-induced liver cell cytotoxicity. It is highly probable that the formation of emodin-cysteine adduct is one main reason for metabolism disorders in emodin treated liver cells, which is related to emodin hepatotoxicity.

Acknowledgments

This work was supported by grants from National Technology Major Project (2014ZX09304307-001-006)

Conflict of interests

The authors declare no conflict of interests.

Notes and references

[a] *Dalian Institute of Chemical Physics, Chinese Academy of Sciences, 457 Zhongshan Road, Dalian 116023, China*
[b]*University of Chinese Academy of Sciences, Beijing 100049, China*
[c]*College (Institute) of Integrative Medicine, Dalian Medical University, Dalian 116044, China*
[d]*College of Pharmacy, Liaoning University of Traditional Chinese Medicine, Dalian 116600, China*
[e]*Institute of Chinese Materia Medica, China Academy of Chinese Medical Sciences, Beijing 100700, China*
***Corresponding author:** Prof. Hongbin Xiao, E-mail: hbxiao69@163.com; Tel: +86 411 8437 9756; Fax: +86 411 8437 9667*

† Electronic Supplementary Information (ESI) available: See DOI: 10.1039/b000000x/

1. J. Xue, W. Ding and Y. Liu, *Fitoterapia*, 2010, **81**, 173-177.
2. Y.-j. Wang, S.-l. Huang, Y. Feng, M.-m. Ning and Y. Leng, *Acta Pharmacologica Sinica*, 2012, **33**, 1195-1203.
3. Q. Huang, G. Lu, H.-M. Sben, M. C. M. Cbung and C. N. Ong, *Medicinal Research Reviews*, 2007, **27**, 609-630.
4. J.-X. Liu, J.-H. Zhang, H.-H. Li, F.-J. Lai, K.-J. Chen, H. Chen, J. Luo, H.-C. Guo, Z.-H. Wang and S.-Z. Lin, *Oncology Reports*, 2012, **28**, 1991-1996.
5. S. O. Mueller, I. Eckert, W. K. Lutz and H. Stopper, *Mutation Research*, 1996, **371**, 165-173.
6. Y.-Y. Chen, S.-Y. Chiang, J.-G. Lin, J.-S. Yang, Y.-S. Ma, C.-L. Liao, T.-Y. Lai, N.-Y. Tang and J.-G. Chung, *Anticancer Research*, 2010, **30**, 945-951.
7. M.-H. Chang, F.-J. Huang and W.-H. Chan, *Toxicology*, 2012, **299**, 25-32.
8. B. H. Ali, S. Al-Salam, I. S. Al Husseini, I. Al-Lawati, M. Waly, J. Yasin, M. Fahim and A. Nemmar, *Fundamental & Clinical Pharmacology*, 2013, **27**, 192-200.
9. X. Wu, X. Chen, Q. Huang, D. Fang, G. Li and G. Zhang, *Fitoterapia*, 2012, **83**, 469-475.
10. J. Yu, J. Xie, X.-j. Mao, M.-j. Wang, N. Li, J. Wang, G.-t. Zhaori and R.-h. Zhao, *Journal of Ethnopharmacology*, 2011, **137**, 1291-1299.
11. S. Peng, L. Yan, J. Zhang, Z. Wang, M. Tian and H. Shen, *Journal of Pharmaceutical and Biomedical Analysis*, 2013, **86**, 56-64.
12. A. Xiong, F. Yang, L. Fang, L. Yang, Y. He, Y. Y.-J. Wan, Y. Xu, M. Qi, X. Wang, K. Yu, K. W.-K. Tsim and Z. Wang, *Chemical Research in Toxicology*, 2014, **27**, 775-786.
13. Z. Huang, G. Chen and P. Shi, *Archives of Pharmacal Research*, 2008, **31**, 742-748.
14. H. Z. Lee, *British Journal of Pharmacology*, 2001, **134**, 1093-1103.
15. M. Acevedo-Duncan, C. Russell, S. Patel and R. Patel, *International Immunopharmacology*, 2004, **4**, 1775-1784.
16. Y.-Y. Chen, S.-Y. Chiang, J.-G. Lin, Y.-S. Ma, C.-L. Liao, S.-W. Weng, T.-Y. Lai and J.-G. Chung, *International Journal of Oncology*, 2010, **36**, 1113-1120.
17. C.-L. Li, J. Ma, L. Zheng, H.-J. Li and P. Li, *Journal of Pharmaceutical and Biomedical Analysis*, 2012, **71**, 71-78.
18. E. Gonzalez, S. van Liempd, J. Conde-Vancells, V. Gutierrez-de Juan, M. Perez-Cormenzana, R. Mayo, A. Berisa, C. Alonso, C. A. Marquez, J. Barr, S. C. Lu, J. M. Mato and J. M. Falcon-Perez, *Metabolomics*, 2012, **8**, 997-1011.
19. B. S. Kumar, B. C. Chung, O.-S. Kwon and B. H. Jung, *Journal of Applied Toxicology*, 2012, **32**, 505-520.
20. X.-m. Chen, J. Liu, T. Wang and J. Shang, *Toxicology in Vitro*, 2012, **26**, 649-655.
21. M. Ma, Z. Jiang, J. Ruan, X. Tan, J. Liu, C. Wang, X. M. Zha and L. Zhang, *Experimental and Toxicologic Pathology*, 2012, **64**, 611-618.
22. L. L. Ji, M. Zhang, Y. C. Sheng and Z. T. Wang, *Toxicology in Vitro*, 2005, **19**, 41-46.
23. K. Dettmer, N. Nuernberger, H. Kaspar, M. A. Gruber, M. F. Almstetter and P. J. Oefner, *Anal Bioanal Chem*, 2011, **399**, 1127-1139.
24. R. Tautenhahn, G. J. Patti, D. Rinehart and G. Siuzdak, *Analytical chemistry*, 2012, **84**, 5035-5039.
25. E. C. Chan, K. K. Pasikanti and J. K. Nicholson, *Nat Protoc*, 2011, **6**, 1483-1499.
26. J. Chen, X. Zhao, J. Fritsche, P. Yin, P. Schmitt-Kopplin, W. Wang, X. Lu, H. U. Haring, E. D. Schleicher, R. Lehmann and G. Xu, *Analytical chemistry*, 2008, **80**, 1280-1289.

27. X. Fu, T. S. Chen, M. B. Ray, H. T. Nagasawa and W. M. Williams, *Journal of Biochemical and Molecular Toxicology*, 2004, **18**, 154-161.
28. H. Sakagami, M. Sugimoto, S. Tanaka, H. Onuma, S. Ota, M. Kaneko, T. Soga and M. Tomita, *Metabolomics*, 2014, **10**, 270-279.
29. X. Shi, D. Yao, B. A. Gosnell and C. Chen, *Journal of Lipid Research*, 2012, **53**, 2318-2330.
30. D. S. Roe, B. Z. Yang, C. Vianey-Saban, E. Struys, L. Sweetman and C. R. Roe, *Molecular Genetics and Metabolism*, 2006, **87**, 40-47.
31. J. G. Okun, S. Kolker, A. Schulze, D. Kohlmuller, K. Olgemoller, M. Lindner, G. F. Hoffmann, R. J. A. Wanders and E. Mayatepek, *Biochimica Et Biophysica Acta-Molecular and Cell Biology of Lipids*, 2002, **1584**, 91-98.
32. M. R. McGill, C. D. Williams, Y. Xie, A. Ramachandran and H. Jaeschke, *Toxicology and Applied Pharmacology*, 2012, **264**, 387-394.
33. J. G. Diaz Ochoa, J. Bucher, A. R. R. Pery, J. M. Zaldivar Comenges, J. Niklas and K. Mauch, *Frontiers in pharmacology*, 2012, **3**, 204-204.
34. G. J. G. Hartmut Jaeschke, Arthur I, Cederbaum, Jack A, Hinson, Dominique Pessayre, John J, Lemasters, *Toxicological Sciences*, 2002, **65**, 166-176.